A comparison of modeled, remotely sensed, and measured snow water equivalent in the northern Great Plains

Thomas L. Mote and Andrew J. Grundstein

Climatology Research Laboratory, Department of Geography, University of Georgia, Athens, Georgia, USA

Daniel J. Leathers

Center for Climatic Research, Department of Geography, University of Delaware, Newark, Delaware, USA

David A. Robinson

Department of Geography, Rutgers University, Piscataway, New Jersey, USA

Received 17 October 2002; revised 9 April 2003; accepted 25 April 2003; published 13 August 2003.

[1] Various methods are available to measure or estimate the quantity of water present in a snowpack. Historically, the National Weather Service has relied on direct measurements taken at first order and cooperative weather stations. Because of the great spatial variability in snow cover density, point measurements are often of limited utility in identifying snow water equivalent (SWE) values over a given area or watershed. Increasingly, remote sensing techniques and physical models have been used to supplement point measurements of SWE and to improve areal estimates of snow water equivalent. This paper compares daily first-order SWE observations from five stations across the northern Great Plains with those estimated from passive microwave remotely sensed data and from an energy and mass balance model (SNTHERM). A commonly utilized SWE algorithm is applied to Special Sensor Microwave/Imager (SSM/I) data across the northern Great Plains during the 1990s. Various filtering algorithms are applied to eliminate those situations in which the SSM/I SWE algorithms are known to be ineffectual. Airborne gamma estimates are also included in the comparison but are limited to only a few observations a year. Although the modeled SWE is generally in good agreement with the observed SWE, there is a tendency for the SNTHERM model to underestimate SWE, but it is typically within the margin of error of the observations. The microwave SWE algorithm apparently overestimates SWE significantly late in the season, compared to in situ observations, likely a result of snow grain growth during snow metamorphism. *INDEX TERMS:* 1863 Hydrology: Snow and ice (1827); 1640 Global Change: Remote sensing; 1878 Hydrology: Water/energy interactions

Citation: Mote, T. L., A. J. Grundstein, D. J. Leathers, and D. A. Robinson, A comparison of modeled, remotely sensed, and measured snow water equivalent in the northern Great Plains, *Water Resour. Res.*, *39*(8), 1209, doi:10.1029/2002WR001782, 2003.

1. Introduction

[2] The unique location and physiography of the northern Great Plains of the United States make it highly susceptible to snow-induced flooding in the late winter and early spring. Throughout the winter, large quantities of snow can accumulate over vast areas. Intrusions of warm air masses in the spring combined with the relatively low relief mean that rapid ablation of the snowpack may occur simultaneously over large areas.

[3] In an attempt to quantify the amount of snow for flood forecasting, the National Weather Service (NWS) operates a network of stations that collect data on the snow water equivalent (SWE), the water content (measured as precipitation) of the existing snowpack. The low station density and the fact that SWE can vary greatly over space make this network insufficient to accurately assess the quantity of snow present across an area. Increasingly, SWE values derived from remotely sensed data and physical models have been incorporated with National Weather Service SWE observations for estimates of regional SWE. It is well known, however, that presently used SWE algorithms applied to remotely sensed observations tend to perform poorly during periods where liquid water or depth hoar (i.e., a layer with ice crystal formation) is present in the snowpack. Similarly, the accuracy of SWE output from physical models is limited to a great extent by the quality of input data. Problems with wind-induced snowfall undercatch can lead to underestimates of SWE.

[4] Given the important role of snow cover in both the hydrology and climate of the northern Plains, the primary objective of this paper is to compare the sources of snow mass information that may be used in assessing SWE. This research compares observed, remotely sensed, and modeled SWE at five first-order NWS stations across the northern Great Plains of the United States. This study utilizes remotely sensed observations of SWE as derived from

0043-1397/03/2002WR001782

SWE algorithms using the Special Sensor Microwave/Imager (SSM/I) instrument and NOAA's airborne gamma instrument as well as modeled SWE from an energy and mass balance model (SNTHERM) to compare to in situ station observations.

2. Data and Methodology

2.1. First-Order in Situ Observations

[5] Daily SWE observations were examined during the winters of 1988–1989 to 1995–1996 from five stations across the northern Plains: Bismarck, Fargo, and Williston, North Dakota, and Aberdeen and Huron, South Dakota. The data were collected from the TD3200/3210 Summary of the Day data set available from the National Climatic Data Center (NCDC) [*NCDC*, 2000a]. SWE observations in this region are typically made by inverting an 8-in precipitation gauge, with a cutting tool attached, into the snow to "cut a biscuit." The melted snow is then poured into a cylinder and measured to the nearest 0.01 in. SWE observations are only required when snow depths are at least 5 cm (2 in). In practice, accumulated water equivalent of snowfall measured in the precipitation gauge is often used to determine SWE for light snowfalls (M. Ewens, personal communication, 2000). While these observations represent some of the best available point measurement coverage across the United States, *Schmidlin* [1990] and *Schmidlin et al.* [1995] have observed a number of problems associated with the accuracy of the data set and a lack of rigorous quality control. They also show that measurements are often taken at locations that are unrepresentative of the surrounding terrain, but the generally uniform terrain of the northern Plains region should mitigate that problem in this study.

[6] Much of the research examining local variation in SWE has focused on complex terrain, such as the mountainous western United States, and may not be applicable to the more uniform terrain of the eastern United States. *Schmidlin et al.* [1995] examined the microscale variation in SWE and found the variability to be 25% on the scale of roughly a hectare, even if great care is taken in the observations at a given time. *Goodison* [1978a] indicated an error range of −0.3 to 12.4% with a mean of 4.6% over a range of SWE of 12–180 mm with the federal standard snow sampler. The standard federal snow sampler has a much smaller diameter than the 8-in gauge used in the northern Plains. It is reasonable to assume that the larger diameter gauge used in the northern Plains would result in smaller errors for shallow snow depths due to the increased area sampled. Variations in snow cover within a region of relatively homogenous climatic conditions are primarily due to differences in land cover or vegetation type [e.g., *Adams*, 1976]. The relatively homogeneous prairie land cover of the northern Plains should minimize the snow cover variability in regions surrounding first-order stations.

[7] Of the in situ SWE observations used for this project, approximately 40–45% were missing during November through April. From records of temperature, precipitation, and snow cover, it is clear that many of these missing data occurred during periods where there was no snow cover present. In most cases, the missing SWE values are in the fall or spring when no snow was present prior to or immediately following a period of low SWE (<15 mm) with temperatures greater than 0°C and little or no precipitation. The missing SWE values often follow SWE observations as low as 3 mm. In these cases it is presumed there was too little SWE for measurement and the missing SWE is replaced with a zero. In instances where there were missing SWE observations between observations showing a substantial snowpack (>15 mm SWE) and no precipitation, linear interpolation was used to estimate the daily SWE values. This process removed more than 90% of the missing values. If a substantial snowpack was in place and precipitation did occur during the period of missing SWE observations, the missing values were not replaced, and those days were not used to calculate the monthly means.

2.2. Cooperative in Situ Snow Depth Observations

[8] Because of the limited spatial coverage of the SWE observations, additional observations of snow depth were collected for NWS cooperative observing stations surrounding each first-order station collecting SWE data. These data are used to determine how representative the SWE measurement is for the surrounding area. *Frei et al.* [1999] and *Kukla and Robinson* [1981] demonstrated that in regions with fairly homogeneous topography, such as the Great Plains, and with multiple cooperative stations per grid cell, the cooperative stations sufficiently represent the spatial variability in snow extent as observed from visible satellite data.

[9] Snow depth data were taken from the NCDC cooperative Summary of the Day data [*NCDC*, 2000b]. Cooperative stations within a 1° latitude × 1° longitude region centered on each first-order station were used to determine a daily average snow depth for the region surrounding each first-order station. We selected cooperative stations that had continuous records with little missing data for the period 1988–1996. Additionally, we attempted to select stations that provided coverage in all directions from the first-order station, even if that resulted in using stations near but outside the 1° × 1° cell (Figure 1). A reasonable coverage was achieved near all first-order stations except Bismarck, where no appropriate cooperative stations were available to the south and southwest.

[10] The snowpack density at the first-order station was then used to convert the average snow depth for the 1° × 1° cell to SWE. The cooperative data were collected to ascertain how representative the observations at the first-order station are for a larger region. In instances where there was a small discrepancy between the first-order and the derived cooperative SWE observations, we assumed the first-order observations were representative of the 1° × 1° cell.

[11] We compared first-order to mean cooperative snow depths on a daily and monthly basis to determine whether the first-order stations are representative of the larger region. For all locations on both a daily and monthly basis, a linear regression of the cooperative snow depths versus first-order snow depths yield r^2 values greater than 0.85, and in most cases greater than 0.90. There was a slight tendency in most cases for the cooperative observations to exceed the first-order, but in all cases this bias was less than 5%. An example figure of the first-order versus mean cooperative monthly snow depths at and around Bismarck, North Dakota, illustrates that the first-order observations are

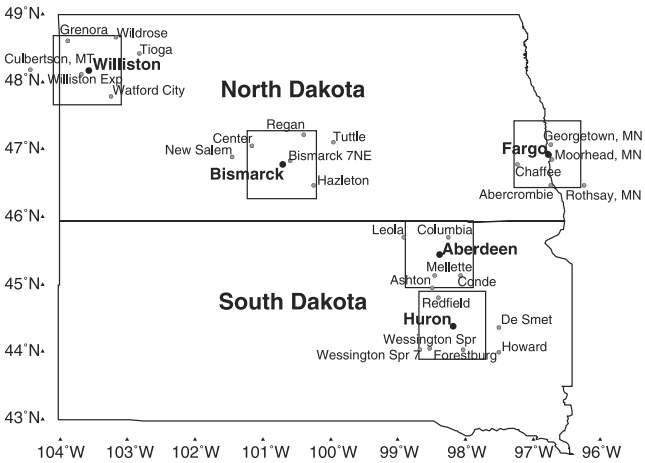

Figure 1. First-order (bold type) and cooperative stations used in this study. The box surrounding each first-order station indicates a 1° latitude by 1° longitude area centered on that station.

generally representative of the 1° × 1° surrounding area (Figure 2).

2.3. SSM/I

[12] The satellite-based microwave data used in this study were the NOAA/NASA Pathfinder SSM/I Level 3 EASE-Grid brightness temperatures, obtained from the EOSDIS National Snow and Ice Data Center (NSIDC) Distributed Active Archive Center (DAAC) at the University of Colorado at Boulder [*NSIDC*, 1999]. This data set, extending from July 1987 to May 1996, was constructed using observations from the Special Sensor Microwave/Imager (SSM/I) mounted on the Defense Meteorological Satellite Program (DMSP) satellite. The SSM/I is a seven-channel, four-frequency passive microwave sensor with brightness temperatures sensed at frequencies of 85.0, 37.0, 22.2, and 19.3 GHz. Brightness temperatures were gridded at a 25 × 25 km resolution at NSIDC.

[13] In this study, the passive microwave brightness temperatures were processed and converted into SWE estimates using an algorithm by the Meteorological Service of Canada (MSC) [*Goodison and Walker*, 1995]. Their method is designed for use in prairie environments and is based on a linear fit between the brightness temperature difference of the 37 GHz and 19 GHz channels with observed SWE, as follows:

$$\mathrm{SWE(mm)} = a + b\Delta T_B \qquad (1)$$

where, for SSM/I, $a = -20.7$, $b = -2.74$, and ΔT_B is the difference between the 37 and 19 GHz vertically polarized brightness temperatures [*Goodison and Walker*, 1995]. Because passive microwave algorithms perform poorly during periods of snowmelt, an algorithm by *Walker and Goodison* [1993] and a version of the algorithm by *Mote and Anderson* [1995] were used to filter out these days. Only overpasses between 0000 and 1200 local standard time (LST) were used to reduce the likelihood of including periods with melting [*Derksen et al.*, 2000c]. A decision tree microwave algorithm for determining land cover type by *Grody and Basist* [1996] was also used to eliminate as many non-snow-covered days as possible. The *Grody and Basist* [1996] decision tree includes categories, among others, for snow, frozen soil, bare unfrozen soil, and open water. *Tait* [1998] demonstrated that even in a terrain similar to the Great Plains with a dry snowpack, an empirical SSM/I algorithm can only estimate SWE to ±44 mm with 95% confidence.

2.4. Airborne Gamma

[14] Another remotely sensed data source for the comparisons are airborne gamma SWE observations conducted by NOAA's National Operational Hydrologic Remote Sensing Center. The observations are instrumental in assessment of SWE for flood forecasting and are taken several times during the season at the request of local NWS offices.

[15] The gamma SWE algorithm relies on the fact that natural emission of gamma radiation by the top 20 cm of the soil is blocked by overlying snow and ice burden [*Carroll*, 2001]. The amount of attenuation is a function of snow mass, not depth. Therefore gamma measurements provide an estimate of SWE but no estimate of snow depth. Background radiation and soil moisture estimates are collected once in the autumn before snow cover is present in order to calibrate each flight line [*Carroll*, 2001].

[16] Each flight line is approximately 16 km long by 0.3 km wide, resulting in a flight line over an area approximately 5 km^2 [*Carroll*, 2001]. Overflights are typically no more than twice a month beginning near the period of peak snowpack. A given flight line would typically have no more than two to three flights per year. The reported root-mean-square error (RMSE) for gamma observations over agricultural land is 8.9 mm, with a bias of approximately 12.1% [*Carroll*, 2001]. Ground-based SWE observations tend to underestimate actual SWE due to difficulty in retaining all moisture in a core, particularly with a depth hoar or ice layer, while gamma SWE may overestimate actual SWE due to superimposed moisture in the soil [*Carroll*, 2001]. An examination by *Schmidlin* [1989] in

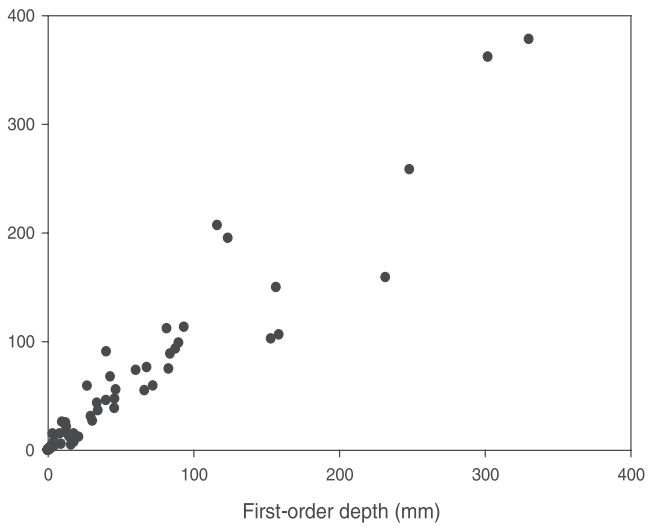

Figure 2. Monthly average first-order versus cooperative snow depth (mean for a 1° × 1° region) for Bismarck, N. D. The linear regression r^2 is 0.92 with a slope of 1.04, indicating slightly larger cooperative depths.

Table 1. Station Anemometer, Gauge, and Thermohygrometer Heights[a]

Station	Anemometer Height, m	Weighing Gauge Height, m	Hygrothermometer Height, m	ASOS Commissioned
ABR (Aberdeen, S. D.)	6.2	1.8	0.9	1 November 1994
BIS (Bismarck, N. D.)	6.2	1.2	1.5	1 May 1996
FAR (Fargo, N. D.)	8.6	7.7	1.5	1 November 1995
HON (Huron, S. D.)	6.2	1.8	1.2	1 November 1996
ISN (Williston, N. D.)	6.2	1.5	1.5	1 April 1996

[a]Compiled from Local Climatological Data annual summaries for 1997; includes only instrument heights from 1987 to ASOS commissioning.

the northern Plains found that gamma SWE estimates generally exceed ground-based SWE estimates.

2.5. SNTHERM

[17] Snowpack modeling is done with SNTHERM, a one-dimensional mass and energy balance model developed at the Cold Regions Research and Engineering Lab (CRREL) [*Jordan*, 1991]. SNTHERM is designed to simulate seasonal snow covers and is one of the more sophisticated models currently available. The model is capable of simulating mass accumulation, ablation, grain growth, and liquid and vapor transmission through the snowpack. The model has been successfully used and tested in a variety of environments across the United States and in Greenland for both climate and hydrological research [*Jordan*, 1991; *Davis et al.*, 1993; *Rowe et al.*, 1995, *Cline*, 1997; *Grundstein and Leathers*, 1998; *Ellis and Leathers*, 1999]. Moreover, this model is of particular interest because it is presently being incorporated into the SNOW-INFO system, operated by a branch of the National Weather Service called the National Operational Hydrologic Remote Sensing Center (NOHRSC) [*Cline and Carroll*, 1999].

[18] The SNTHERM surface energy balance at the surface-atmosphere interface includes radiative fluxes, turbulent energy fluxes, and convected energy due to snowfall or rainfall. These terms are expressed in the following equation:

$$I_{\text{top}} = I_s \downarrow \left(1 - \alpha_{\text{top}}\right) + I_{ir} \downarrow - I_{ir} \uparrow + I_{\text{sen}} + I_{\text{lat}} + I_{\text{conv}} \qquad (2)$$

where I_{top} is the net surface energy budget at the surface-air interface, $I_s\downarrow$ is the downward directed solar radiation, α_{top} is the surface albedo, $I_{ir}\downarrow$ and $I_{ir}\uparrow$ are the downward and upward components of longwave radiation respectively, I_{sen} and I_{lat} are sensible and latent heat fluxes respectively, and I_{conv} is the energy convected by rain or snowfall [*Jordan*, 1991].

[19] Because of the lack of observed radiation data, algorithms supplied in the model were used to compute the shortwave and longwave radiative fluxes. Incoming solar radiation is estimated based on a three-level insolation model by *Shapiro* [1987] that breaks the atmosphere into levels corresponding to low, middle, and high clouds [*Jordan*, 1991]. Solar radiation incident on the surface is the net result of transmission and reflectance within each of the three layers and is given by

$$I_s \downarrow = \frac{\tau_1 \tau_2 \tau_3}{D} I_{s00} \qquad (3)$$

where τ_1, τ_2, and τ_3 are the transmissivities of the three different layers of the atmosphere, D is a constant based on transmission and reflectance, and I_{s00} is the solar radiation at the top of the atmosphere [*Jordan*, 1991]. Outgoing longwave radiation is computed using the Stefan-Boltmann equation, while downwelling longwave radiation is determined using an empirically based equation by *Idso* [1981] that relies on surface air temperature and vapor pressure. Latent and sensible heat fluxes are calculated using bulk aerodynamic equations [*Jordan*, 1991].

[20] Elements of the energy balance equation are driven by inputs of meteorological data. First-order NWS data for temperature, relative humidity, wind speed, cloud height, cloud cover percentage, and cloud type were obtained from the National Climatic Data Center (NCDC) Surface Airways database. Five stations with long and complete periods of record from 1949 through 1996 were used in the study (Table 1). For computation of turbulent energy exchange, the measurement heights for temperature, relative humidity, and wind speed were needed. These values correspond to the sensor heights at first-order NWS stations (Table 1).

[21] The first phase of the modeling effort involved constructing complete data sets at a 1-hour temporal resolution. First-order NWS observations are generally taken at hourly intervals, but for short periods where individual hourly observations were not available, temperature, relative humidity, and wind speed were estimated using an Akima cubic spline interpolation routine [*Akima*, 1970].

[22] The algorithms for computing solar and longwave radiation require information on cloud type and cloud height. Missing cloud height data were estimated using a convective cloud base scheme [*Ahrens*, 1994]. The model recognizes five different cloud types corresponding to different heights in the atmosphere. Low clouds include cumulus/cumulonimbus and stratus/stratocumulus, middle level clouds are altostratus/altocumulus, and high-level clouds are cirrus and cirrostratus [*Jordan*, 1991]. For periods when these data were not available, they were estimated from cloud height and the percentage of cloud cover.

[23] The calculation of incoming solar radiation also requires information on the latitude, longitude, slope and azimuthal angles, and time of day. The surface of the study region is assumed to be nearly flat, which simplifies the modeling process by eliminating the need for inputs of slope and azimuth.

[24] The physical characteristics of the soil and snow layers were set based on previous work by *Jordan* [1991]. A variable albedo algorithm based on the work of *Marshall*

and Warren [1987] was utilized for the snow cover, while a constant albedo of 0.2 was set for bare soil. The variable albedo algorithm adjusts the albedo of the snowpack as grain size changes during the long-term metamorphism of the pack. The bare soil albedo was selected to account for the presence of grass and fallow crops as well as to provide a middle value between a dark, wet soil and a light, dry soil. The soil medium is set as sandy soil that is 1 m deep; it is then divided into nine layers of varying thickness. The model was run at each of the five stations beginning in the summer with initial thermal and moisture conditions specified only for soil layers.

2.6. SNTHERM Precipitation and Under-Catch Correction

[25] In order to accurately model SWE, the most critical factor in using SNTHERM is to add the proper amount of precipitation into the model. The role of SNTHERM is primarily to ablate the accumulated snowfall at the proper time and in the proper amount given the prevailing meteorological conditions. SNTHERM requires precipitation values in units of water equivalent; these data were obtained from an NCDC data set compiled from hourly precipitation observations. Because the hourly precipitation type was not readily available for all stations in this region during the entire time period, the precipitation type was determined based on surface air temperature. The precipitation is considered snow if the air temperature was at or below 0°C. Otherwise the precipitation was assumed to be rain. *Yang et al.* [1997] found that a 0°C rain/snow cutoff worked best for modeling SWE using the Biosphere-Atmosphere Transfer Scheme (BATS). *Lynch-Stieglitz* [1994], for a snowmelt and sublimation model for the GISS GCM, also used 0°C as the rain/snow threshold temperature. Because SNTHERM requires a single precipitation type, no mixed precipitation category was included. The model was also set to compute the densities of newly fallen snow. SNTHERM was modified to use a function based on a NWS operational procedure that determines the approximate density of newly fallen snow from air temperature. The bulk density of falling snow was set categorically by temperature range, and decreases with temperature [*NWS*, 1996].

[26] Precipitation gauges have a systematic bias, particularly with snowfall, that leads to underestimates of precipitation [e.g., *Goodison*, 1978b; *Legates and DeLiberty*, 1993]. This ''under-catch'' is due largely to the effect of the wind, but also includes losses due to wetting of the snow inside the gauge and the accumulation recorded as a trace. Losses as large as 40 percent can occur during the winter due to under-catch [*Legates and DeLiberty*, 1993]. Of these losses, by far the most significant is the wind-induced under-catch [*Yang et al.*, 1998]. The losses due to wetting and through trace accumulation are ignored in this study. After contacting several Data Acquisition Program managers (DAPMs) at the National Weather Service forecast offices in the region, it was determined that all of the precipitation gauges used in this study were Universal gauges shielded with an Alter type shield during the period of study. An appropriate under-catch correction factor was used that accounted for the shielding.

[27] The under-catch correction is based on the relationship between the under-catch fraction and the wind speed at the gauge height. The wind speed at the gauge height was not available and required the reduction of wind speed from the anemometer height to the precipitation gauge height by assuming a logarithmic wind profile [*Rosenberg et al.*, 1983]. The precipitation gauge heights and anemometer heights for the stations are shown in Table 1. A typical surface roughness for a snow-covered surface is given as 0.01 m [e.g., *Yang et al.*, 1998]. *Larson* [1971] arrived at a roughness length of 0.0065 m for a snow-covered location near Laramie, Wyoming. The corrections shown here assume a surface roughness of 0.01 m. (The difference in wind speed calculated at gauge height using roughness lengths of 0.01 m and 0.0065 m was nearly always much less than 0.1 m s^{-1}. The typical difference in storm total accumulation using the two suggested roughness lengths was nearly always much less than 5% and within the error of the under-catch corrections and precipitation measurement. Therefore the difference in suggested roughness lengths is deemed not to be a significant factor in gauge-corrected precipitation totals.)

[28] The under-catch correction used here was that developed by *Goodison* [1978b], who compared the Canadian Nipher shielded snow gauge to Universal (Belfort) and Fischer and Porter gauges. He gives the catch ratio (CR) for the Universal gauge as

$$\mathrm{CR} = e^{0.0055 - 0.133\,w} \tag{4}$$

where w is the storm-average wind speed. Events with storm-average wind speeds exceeding 6 m s^{-1} were treated as having a wind speed equal to 6 m s^{-1} for the purpose of gauge correction. Higher wind speeds are often associated with some blowing snow accumulation in the gauge, offsetting some of the loss of captured accumulation [*Goodison*, 1978b; *Yang et al.*, 1998]. A catch ratio for Alter-shielded Belfort gauges as part of the World Meteorological Organization's Solid Precipitation Intercomparison project is presented by *Yang et al.* [1999], but the catch ratios do not account for variation in wind speed of individual storm events. Given differences in mean wind speeds of storm events for the stations used in this study, the *Yang et al.* [1999] catch ratios were not used.

[29] Since storm-averaged wind speeds were used by *Goodison* [1978b], storm-averaged wind speeds are used here by calculating the mean wind speed during the period of snowfall. The storm-averaged wind speed is used only for correcting snowfall. The hourly wind speeds are used as the wind input to drive SNTHERM. Appropriate under-catch corrections for Alter shielded Universal gauges from *Goodison* [1978b] were used for rainfall events as well.

2.7. Spatial Representativeness

[30] One of the primary difficulties in comparing surface point observations, model output, and airborne and satellite remote sensing is the spatial representativeness of each measurement. This problem is common in a variety of research efforts, most notably any remote sensing validation studies. The surface observations are only valid at a single point, and it is uncertain how representative those observations are of a larger surrounding region. The remotely sensed observations are integrated measurements over some area. The SNTHERM model runs are not truly point- or

area-averaged observations. Meteorological data input into SNTHERM, such as temperature and humidity, is likely representative of a larger area than the immediate vicinity of the meteorological station. Much of the meteorological data used to drive SNTHERM (e.g., temperature and humidity) typically show smaller variation than precipitation across a region the size of a 1° × 1° cell. However, because of the greater spatial variability in precipitation measurements, the model is likely more similar to the manual SWE measurements.

[31] As a means for comparing the SWE observations, a common spatial area was selected. A 1° latitude by 1° longitude region centered on each first-order station was used for the comparison. The snow depths from cooperative observers were averaged for the same 1° × 1° region and converted to SWE, as discussed in the previous section, for assessing the representativeness of the first-order SWE observations. The SSM/I SWE estimates were averaged over this region. Typically, 12 to 16 EASE grid cells are included in each 1° × 1° region. Moreover, the airborne gamma flight lines within each 1° × 1° region were averaged. Any lines that were flown in a 5-day window surrounding the day of interest were included in the average. In most cases, only a few lines were available. While these lines may not represent the entire 1° × 1° region, we are limited by the relative paucity, compared to the other data sources, of airborne gamma overflights. The SNTHERM model runs are based on meteorological observations from the first-order station.

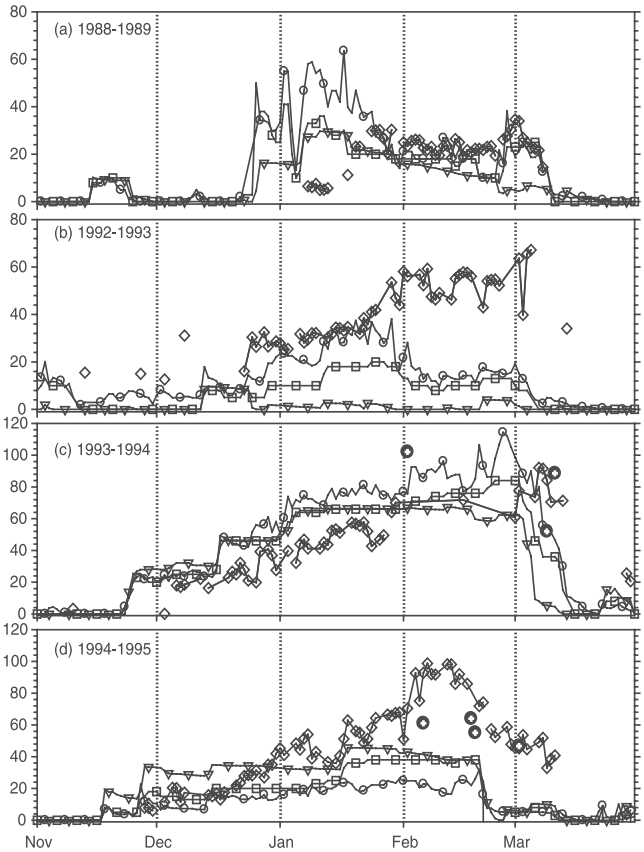

Figure 3. Snow water equivalent (mm) time series for Bismarck, N. D., from first-order National Weather Service station measurements (squares), 1° latitude × 1° longitude average SSM/I (diamonds), SNTHERM output (downward triangles), cooperative snow depth-derived SWE (circles), for (a) 1998–1989, (b) 1992–1993, (c) 1993–1994, and (d) 1994–1995. First-order, cooperative and SNTHERM SWE symbols shown only every fifth day.

3. Intercomparison of SWE

[32] The use of SNTHERM and SSM/I estimates of SWE, as well as collection of the limited in situ SWE observations, is part of a larger project to develop a climatology of SWE for the grasslands regions of North America and Eurasia. The blending of these data sets will require a careful analysis of the strengths and weaknesses of each data set. Comparisons at Bismarck, Fargo, and Williston, North Dakota, and Huron and Aberdeen, South Dakota, have been completed. Example time series showing observed SWE, SNTHERM, and SSM/I estimated SWE are shown in Figure 3. In the future, it may be possible to improve upon this error by combining SNTHERM and satellite remote sensing to improve the estimates from both, such as work done by *Wilson et al.* [1999]. In that work, the SNTHERM output is used to improve SSM/I SWE algorithm. This may be one means of "blending" the data sets.

3.1. SNTHERM

[33] We begin the discussion by examining the SNTHERM runs for each station using the *Goodison* [1978b] precipitation under-catch corrections. Comparison between SNTHERM-derived SWE and observed SWE are made on a seasonal and mean monthly basis. A comparison is also made on a daily basis, with the addition of airborne Gamma estimates of SWE, for the following winters: 1988–1989, 1992–1993, 1993–1994, and 1994–1995. Those winters were selected because little snow cover was present at most of the stations during the winters of 1989–1990, 1990–1991, and 1991–1992. The winter of 1995–1996 had limited snow cover at the South Dakota stations. Comparisons are made primarily with the first-order SWE observations. Since the SNTHERM SWE output is based on input meteorological data from the same first-order site, it is appropriate to compare the SNTHERM SWE output to the independent first-order SWE observations.

3.1.1. Seasonal

[34] The first comparison was made on seasonal (November–April) average SWE. While snow cover is often absent during November and April, sufficient snow cover exists at some of the stations used in the study such that those months were included for the sake of consistency.

[35] In general, the agreement in average SWE among the three data sets is quite good, although the standard deviations are quite large. At Aberdeen, Bismarck, Williston, and Huron, the seasonal observed SWE is within 3 mm of the SWE estimated from the SNTHERM runs (Table 2). However, it should be noted that the mean observed SWE (November–April) at Huron is only 5.9 mm.

[36] Only at Fargo is the difference between the observed SWE and SNTHERM output SWE large. The mean seasonal observed SWE is 21.1 mm, while the SNTHERM runs yield mean SWE of 15.1 mm (Table 2). The SNTHERM SWE is in much closer agreement with the cooperative-derived SWE. There are two unique features to

Table 2. Mean Monthly and Seasonal SWE From SSM/I, First-Order Station Observations, Cooperative Snow Depths (Using Snow Density From First-Order Stations), and SNTHERM Model Output

	SSM/I	Observed	Cooperative	SNTHERM
		Aberdeen		
Nov.	1.59	1.75	3.35	0.98
Dec.	8.04	7.85	10.24	5.10
Jan.	18.30	16.38	17.92	13.49
Feb.	21.04	16.54	16.82	11.16
March	15.05	8.07	7.23	9.66
April	0.55	0.06	0.56	0.23
Season	9.70	8.36	9.63	6.08
		Bismarck		
Nov.	4.06	3.99	4.15	10.91
Dec.	8.84	8.98	8.42	14.46
Jan.	22.07	20.28	21.72	21.14
Feb.	25.02	18.34	18.96	15.68
March	12.19	5.24	6.73	4.18
April	0.54	0.59	0.88	1.51
Season	11.85	10.27	10.65	12.64
		Fargo		
Nov.	0.82	3.97	4.09	3.38
Dec.	6.51	13.47	10.50	13.51
Jan.	18.51	38.81	29.27	26.65
Feb.	31.56	51.26	26.36	30.78
March	32.96	26.54	13.11	25.55
April	1.47	0.87	0.75	2.39
Season	11.44	21.13	13.93	15.06
		Huron		
Nov.	0.94	0.67	1.80	0.95
Dec.	6.00	3.45	5.43	3.29
Jan.	13.43	11.29	12.38	7.92
Feb.	13.13	14.44	13.90	10.00
March	4.45	2.61	3.37	6.29
April	0.18	0.41	0.79	0.59
Season	6.61	5.90	6.72	4.45
		Williston		
Nov.	2.05	0.91	2.59	2.05
Dec.	8.82	4.55	6.39	4.73
Jan.	21.84	16.03	15.09	14.74
Feb.	22.41	15.46	10.03	14.94
March	7.70	4.18	3.12	4.08
April	0.89	0.00	0.58	0.41
Season	10.98	7.23	6.85	7.22

the observations made at Fargo. First, the precipitation gauge was located on a building rooftop at 7.7 m. The wind speed estimated at gauge height is higher than at other stations for the same recorded wind speed. The result is a greater under-catch correction than at other sites. The result should be an increase in SNTHERM estimates of SWE than would be expected at other sites. However, the SNTHERM SWE estimates are lower than the observed SWE. Additionally, SWE observations for Fargo were taken by a cooperative observer in Moorhead, Minnesota. The data for Fargo should be used with caution but are retained in this study to demonstrate the significance of the siting of SWE and precipitation observations.

3.1.2. Monthly

[37] At the stations used in this study, the deepest snow cover is typically during January and February, while snow is seldom present at even the northern stations in October or May. Therefore it can be more instructive to examine the differences between the corrected observed SWE and the three SNTHERM model runs by month.

[38] During the months of January and February, which had the greatest average SWE at all stations, the mean monthly SNTHERM SWE was nearly always less than the observed SWE. Given that the observed SWE is generally assumed to be an underestimate of the true SWE, the SNTHERM estimates are also likely underestimates of actual SWE.

3.1.3. Daily

[39] There is no clear systematic bias when examining the daily SNTHERM SWE versus the observed SWE. While the SNTHERM SWE is often lower than the observed SWE, it is often within the error of the observed SWE. In many cases, the SNTHERM estimates of SWE nearly match the observed SWE values. For example, difference between the SNTHERM SWE and observed SWE is well within the 25% microscale error of the SWE observations [*Schmidlin et al.*, 1995], as well as error in precipitation measurements and under-catch correction, at Bismarck during January and early February of 1989, 1994, and 1995 (Figures 3a, 3c, and 3d).

[40] Only during the midwinter of 1992–1993 is the SNTHERM estimate substantially less than the observed SWE (Figure 3b). It is important to note that the SWE observations are quite low at this time (<20 mm). This difference seems most pronounced after precipitation events during 28 December 1992 and 12 January 1993. The total precipitation during the 28 December and 12 January events, corrected for gauge under-catch, was approximately 8 mm of water equivalent, yet the observed SWE increased 10 mm. The SNTHERM SWE for the same period increased only 2.8 mm. SNTHERM sublimated much of the snowfall accumulation from 28 December before the 12 January snowfall event occurred. Conditions between 28 December and 12 January were relatively cold and dry, with temperatures exceeding −10°C only one day.

[41] A similar pattern is evident at Williston, where January to early February of 1989, 1994, and 1995 demonstrate a good match between SNTHERM and the observed SWE (Figures 4a, 4c, and 4d), while SNTHERM SWE is lower during the midwinter of 1992–1993 (Figure 4b). At Aberdeen, SNTHERM shows substantially more SWE than observations in January and February of 1989 (Figure 5a), while other years show a much closer correspondence, within the error of the surface observations (Figures 5b, 5c, and 5d).

[42] There is a tendency in several years for SNTHERM to substantially underestimate SWE, compared to surface observations of SWE at the first-order stations, in late February and March, just prior to spring melt. Clear examples can be seen at Bismarck in 1989 and 1994 (Figures 3a and 3c), Williston in 1994 (Figure 4c), and Aberdeen in 1993 and 1994 (Figures 5c and 5d).

3.1.4. Evaluation

[43] SNTHERM seems to adequately capture the seasonal mean SWE and seasonal cycle at four of the five stations in this study. The exception is Fargo, which has peculiarities in the location of the SWE observation that likely plays a large role in the difference. This is particularly evident when comparing the SNTHERM SWE to the SWE estimate from

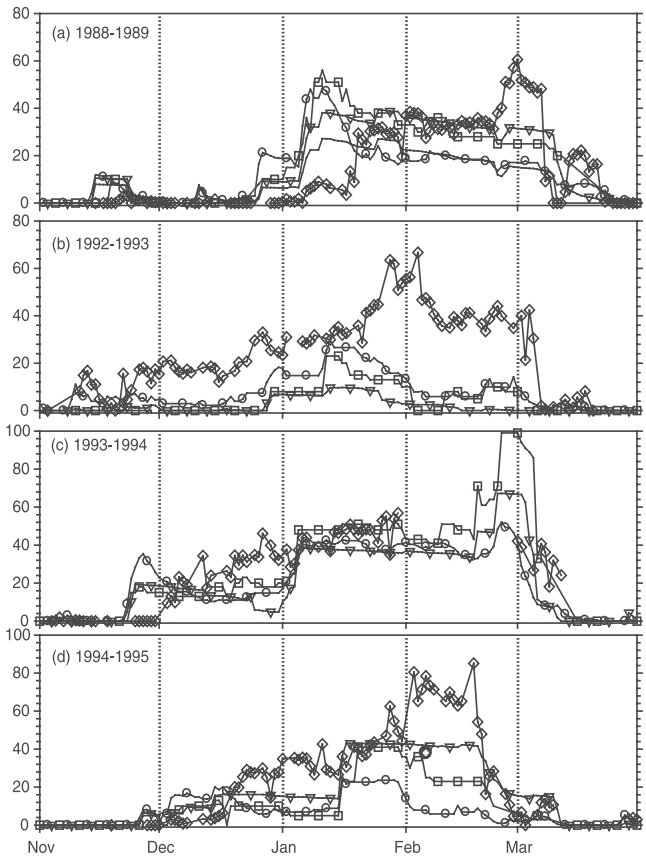

Figure 4. Same as Figure 3, but for Williston, N. D.

the cooperative depth observations for the 1° × 1° region surrounding Fargo. Overall, there is a tendency for SNTHERM to underestimate SWE, compared to surface observations. This is especially significant given that surface observations are generally assumed to be underestimates of actual SWE. Most important, the differences between the SNTHERM SWE estimates and station observations of SWE are generally within the error of the SWE observations.

3.2. SSM/I

[44] The seasonal mean, monthly mean, and daily SWE estimates from SSM/I using the Canadian MSC algorithm were also compared to surface observations of SWE, cooperative snow depth-derived estimates of SWE, and airborne Gamma estimates of SWE. The SSM/I SWE estimates are averaged for EASE grid cells within a 1° latitude × 1° longitude region surrounding each first-order station, as described previously.

[45] The MSC SSM/I SWE algorithm is based on fieldwork in Saskatchewan where airborne multichannel passive microwave instrument was compared to ground and airborne gamma surveys [*Goodison et al.*, 1986]. Attempts to assess the error of the MSC SWE algorithm yield SSM/I SWE estimates within 10–20 mm of surface measurements for dry snow conditions in the Canadian prairies [*Goodison*, 1989]. The immediately adjacent regions in the United States, with similar agricultural uses, are considered in this study. Periods with wet snow are filtered out as much as possible. Moreover, *Derksen et al.* [2000a, 2000b] have employed the MSC SSM/I SWE algorithm over the northern Plains of the United States. Nevertheless, with no prior knowledge of snow conditions, it is likely the error is on the higher end of the 10–20 mm range or closer to the 44-mm error given by *Tait* [1998].

[46] The SSM/I-derived SWE values represent an area average of several 25 km EASE grid cells within a 1° latitude × 1° longitude region. It may not be appropriate to compare the SSM/I-derived SWE with the first-order SWE, particularly if the snow depth at the first-order station is significantly different than the snow depths at surrounding cooperative stations within the 1° × 1° region. As described in 2.2, we created SWE estimates based on snow density at the first-order site and average snow depths from cooperative stations within the 1° × 1° region. If the cooperative-derived SWE is similar to the first-order SWE, it indicates that the first-order site is likely representative of the 1° × 1° region. In this section, both the cooperative-derived and first-order SWE are compared to the SSM/I-derived SWE.

3.2.1. Seasonal

[47] The SSM/I also provides SWE estimates that are similar in magnitude to the first-order and cooperative-derived SWE at four of the five stations. The differences are less than 2 mm at Aberdeen, Bismarck, and Huron and less than 3 mm at Williston (Table 2). Only at Fargo is the difference between the mean seasonal SSM/I and the first-order observed SWE substantial (11.4 and 21.1 mm, respectively). However, the SSM/I estimate is within 2 mm of

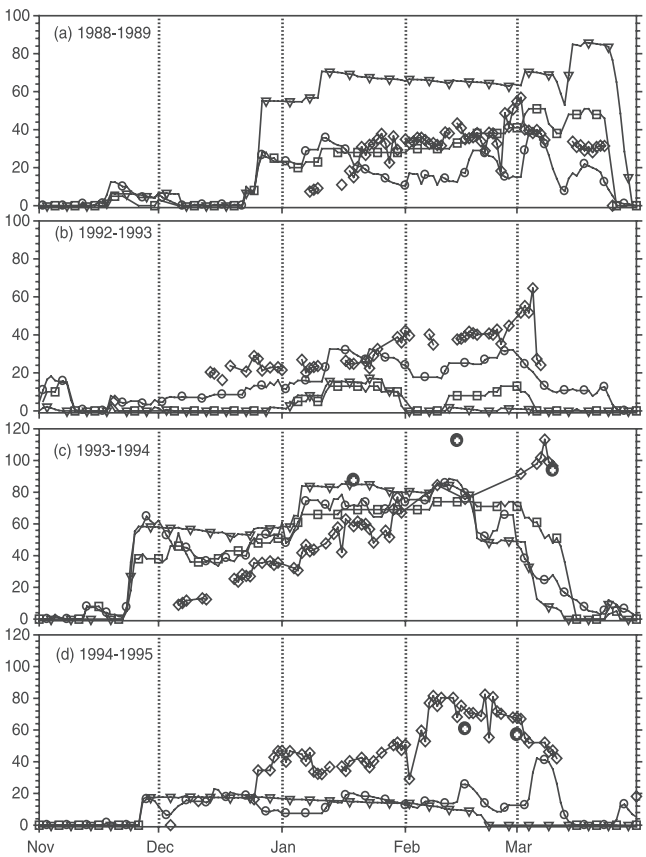

Figure 5. Same as Figure 3, but for Aberdeen, S. D.

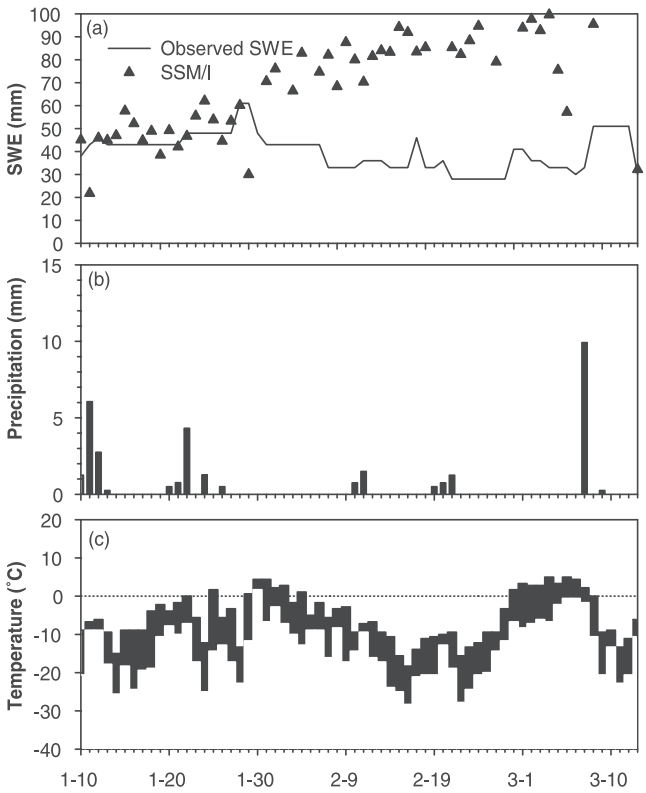

Figure 6. (a) Daily SWE observations and SSM/I SWE estimates and (b) precipitation and (c) daily temperature range during 1992–1993 at Fargo, N. D.

the cooperative-derived SWE and within 4 mm of the SNTHERM SWE estimate at Fargo (Table 2).

3.2.2. Monthly

[48] The SSM/I shows a strong correspondence to the observed SWE during many months. For example, during December and January at Bismarck, the cooperative-derived SWE is 8.4 mm and 21.7 mm, respectively, while the mean SSM/I SWE is 8.8 mm and 22.1 mm, respectively (Table 2). The same months at Huron show an average cooperative-derived SWE of 5.4 mm and 12.4 mm, respectively, while SSM/I shows 6.0 mm and 13.4 mm (Table 2). December and January at Aberdeen have an average cooperative-derived SWE of 10.2 mm and 17.9 mm, while the average SSM/I SWE for the 1° × 1° region is 8.0 mm and 18.3 mm (Table 2).

[49] The SSM/I substantially overestimates SWE compared to the cooperative-derived and first-order SWE at Williston during January and February by 6.7 mm (44%) and 12.4 mm (123%), respectively. The SSM/I also substantially overestimates SWE compared to surface observations at most stations late in the season, particularly in March. For example, the March SSM/I SWE is greater than the cooperative-derived SWE by 7.8 mm (108%) at Aberdeen, 5.5 mm (81%) at Bismarck, 1.1 mm (32%) at Huron, and 4.6 mm (147%) at Williston. The reason for this discrepancy will be explored at length in the next section.

[50] The only station that has substantially lower SSM/I SWE estimates than surface observations is early in the season at Fargo. For example, the cooperative-derived SWE is 29.3 mm in January (first-order observations average 38.8 mm), while SSM/I shows 18.5 mm (−37%) (Table 2). During February and March, Fargo exhibits the same pattern as the other stations with SSM/I showing more SWE than surface observations. This pattern at Fargo is also explored in the next section.

3.2.3. Daily

[51] In the daily time series, it is evident that the SSM/I has a pattern of relatively accurate SWE early through the middle of the winter and overestimating SWE late in the season compared to the first-order and cooperative-derived. During the early to middle of the winter, the SSM/I and surface observations agree well within the margin of error for each. For example, during January of 1994 at Bismarck (Figure 3c) and Williston (Figure 4c), January 1995 at Williston (Figure 4d), and January of all years at Aberdeen (Figure 5), there is good agreement between SSM/I and surface observations.

[52] In some cases, the SSM/I overestimation of SWE on a daily basis is greater than 100% late in the season. This is clear in February 1993 and 1995 at Bismarck (Figures 3b and 3d), Williston (Figures 4b and 4d), and Aberdeen (Figures 5b and 5d). Figures 6 and 7 show detailed examples of the SSM/I overestimates late in the season.

[53] There may be a systematic underestimate in the SSM/I at Fargo early in the season due to forest cover. The EASE-Grid footprint surrounding Fargo has approximately 20% forest cover due to riverine forests, particularly along the Red River, urban forests within Fargo, and a substantial number of shelter belts planted along the margins of farm fields. None of the other four locations has significant forest cover. Forest cover can reduce the micro-

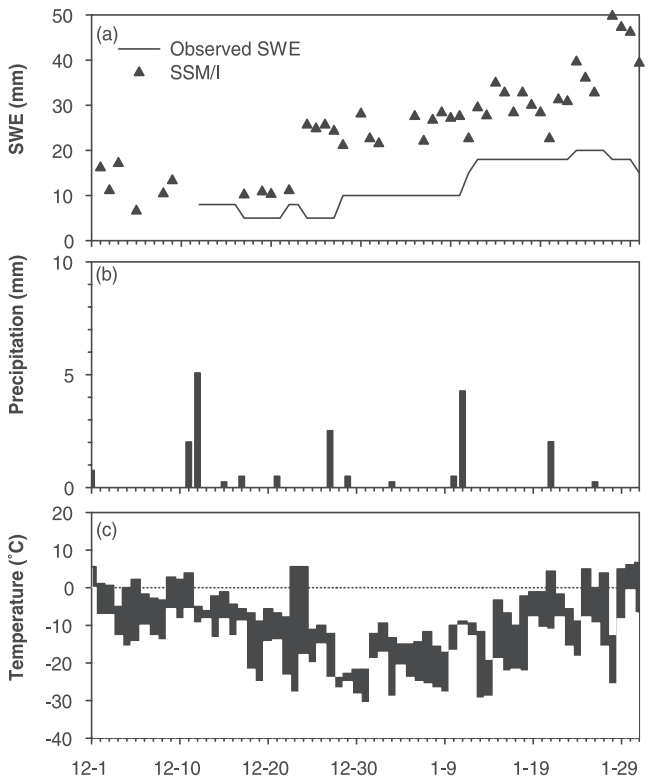

Figure 7. (a) Daily SWE observations and SSM/I SWE estimates and (b) precipitation and (c) daily temperature range during 1992–1993 at Bismarck, N. D.

wave SWE estimates by reducing the frequency difference between 19 and 37 GHz due to the emission of microwave radiation from the forest canopy [*Hall et al.*, 1982; *Chang et al.*, 1990, 1991, 1996]. This effect could have created the SWE underestimate typical early in the season at Fargo compared to both the first-order and the cooperative-derived SWE.

[54] In many instances, the SSM/I overestimation late in the season was due to a prolonged period with little snow, often after a midwinter melt event, with substantial densification and grain growth in the near-surface layers. Larger grain sizes reduce the overall emissivity of the snowpack. This grain growth also increases the frequency gradient (difference in 19 and 37 GHz brightness temperatures) and creates the appearance of increased SWE. During January and February 1993, an example of such an event occurred at Fargo. From 12 to 25 January 1993, the average observed SWE was 44.3 mm while the SSM/I SWE was 46.9 mm (Figure 6a). From 25 January to 5 February 1993, a series of days occurred with temperatures above freezing and no precipitation (Figures 6b and 6c); the warmest day, 31 January, had a maximum temperature of 4.4°C and a minimum of 1.7°C. After 5 February, the temperatures did not exceed freezing until 1 March and only 4.8 mm of precipitation fell (Figure 6b). The coldest day, 17 February, had a maximum temperature of −18.3°C and a minimum temperature of −28.3°C. During this period of below 0°C weather, the mean observed SWE was 33.8 mm while the SSM/I SWE was 65.8 mm (Figure 6a). These comparisons assume that the meteorological data recorded at Fargo are representative of the surrounding region, an assumption with is supported by cooperative observations during this period in the 1° × 1° region surrounding Fargo.

[55] A similar example can be found during the same winter at Bismarck. On 23 December 1992, the SSM/I estimated 11.1 mm of SWE at Bismarck while the observation on that date showed 8 mm. Snowfall on 11–13 January 1993 increased the observed SWE to 18 mm, but by 23 January the SSM/I estimate was 31.2 mm (Figures 7a and 7b). This corresponds to a period with almost no precipitation and cold temperatures (Figures 7b and 7c). After a maximum temperature of 5.6°C on 25 December 1992, temperatures did not exceed freezing until 26 January 1993, with maximum temperatures as low as −19°C and minimum temperatures as low as −29°C (Figure 7c). In both cases, a much steeper frequency gradient results in the apparent overestimation of SWE by SSM/I. The SNTHERM stratigraphy output (not shown) indicates that significant grain growth and densification in the near surface layers from the strong temperature gradient introduced into the snowpack resulted in this steeper SSM/I frequency gradient. SNTHERM indicates grain growth from approximately 0.5 mm to 2.5 mm in the top few centimeters of the snowpack during that time. Although the absolute grain sizes in SNTHERM may not be correct, the relative change is probably realistic.

[56] However, it should also be noted that during these periods when SSM/I was much higher than observed SWE, it was often much closer to airborne Gamma estimates of SWE for flight lines within the 1° × 1° region. During late February and early March of 1995, the SSM/I estimates of SWE are of the order of 50 mm, compared to surface observations dropping to 5–10 mm, while the airborne gamma estimates are nearly identical to the SSM/I. Another example at Bismarck in March of 1997 (not shown) has observed SWE of 30–50 mm, SSM/I near 80 mm, and gamma 90–110 mm.

3.2.4. Evaluation

[57] There is good reason to be cautious about comparing an observation at a single point with a satellite sensor that is nominally integrating over an area larger than 600 km^2 or a model that is probably more representative of an areal average. One of the difficulties in employing SSM/I or other passive microwave instruments for measuring SWE is the tendency for empirical algorithms to be sensitive to changes in the snowpack's structure over the course of the season. All of the existing operational microwave algorithms, including the MSC algorithm employed in this paper, rely on the increase in scattering with increasing snow mass. However, the scattering and emission signatures of snowpacks are also sensitive to changes in snowpack density, grain size, and water content. The best approach to estimate SWE with existing SSM/I algorithms may be to simply not use the algorithm when conditions indicate large changes in snow grain size and snow density or the presence of liquid water in the pack. Liquid water so dramatically reduces the volume scattering of the snow that it is likely impossible to derive any useful SWE estimates from a melting snowpack.

[58] In early to midseason, the SSM/I seems to agree well with surface observations taken at Huron, Aberdeen, and Bismarck. There is a clear discrepancy late in the season when SSM/I shows substantially more SWE than the in situ observations, but is often much closer to the airborne gamma SWE measurements. It is important to note that the Canadian MSC SSM/I SWE algorithm was developed with airborne gamma validation and in locations in Saskatchewan that have conditions more similar to the cold and dry periods, and located closer to Williston. These are the same circumstances where we see SSM/I overestimates compared to surface SWE observations. If the airborne gamma is a better measurement of SWE than the in situ observations, it may be true that the SSM/I is underestimating SWE early in the season and is closer to correct late in the season. It may be simply that the locations where the first-order SWE observations are taken (e.g., airports) are more likely to see more rapid melting in the spring. Regardless, this discrepancy late in the season deserves further examination.

4. Conclusion

[59] Many approaches are currently used to obtain estimates of SWE; each method has advantages and disadvantages depending on the application. Multiple sources of SWE information are often used operationally, yet few comparisons have been of the relative values of the different sources of SWE information. One of the difficulties of such a comparison is the difference in spatial scales of the measurements. In this research, we have selected a study region in which the scale problem is minimized because of the relative homogeneous nature of the region. While the authors recognize the incongruity in comparing observations taken at various spatial scales, we also recog-

nize that these data sources are regularly utilized in assessing snow mass.

[60] A comparison of National Weather Service observations of SWE with modeled SWE from SNTHERM in general reveals good overall agreement for the locations examined in the northern Great Plains. The agreement between SNTHERM estimates of SWE and point observations increases substantially after applying an appropriate under-catch correction to the precipitation data used in SNTHERM. There is some tendency of SNTHERM to underestimate SWE compared to in situ observations of SWE.

[61] Overall, the SSM/I using the Canadian MSC SWE algorithm compares well with in situ observations in December and January at three of the stations but appears to overestimate SWE late in the season. At only one location, Fargo, North Dakota, did the SSM/I typically underestimate the SWE. We believe this is at least due partially to some forest cover in the region, which was not accounted for in this study but does influence the microwave emission of the landscape. The large overestimation by SSM/I late in the season may be due to snow grain growth from (1) melt-freeze metamorphism and (2) the introduction of large temperature gradients into the snowpack during cold weather. This would likely be true of any existing passive microwave SWE algorithm and is not a unique problem to the MSC algorithm. Comparisons with airborne gamma SWE indicate that in situ observations may simply underestimate actual SWE late in the season.

[62] The results indicate that on a daily, monthly, and seasonal basis, SNTHERM can provide a reasonable estimate of measured SWE, after accounting for precipitation under-catch, but there is some tendency to underestimate SWE early in the season. Conversely, SSM/I can provide reasonable estimates of SWE during the coldest months, except during periods of depth hoar, but is less useful in spring when compared to in situ observations. These results underscore the need for combining all of the available sources of SWE when attempting to produce climatological estimates of snow mass, which is the current direction for this research. These climatological estimates of SWE should prove valuable in validating general circulation model (GCM) simulations, understanding large-scale variability in climate and hydrology, and in serving as a baseline for operational hydrology.

[63] **Acknowledgments.** This work was partially supported by NASA Land Surface Hydrology Program grant NAG5-8469 and NASA GAPP Program grant NAG5-11592. Thanks to Tom Carroll of NOHRSC, Richard Armstrong of the University of Colorado, and an anonymous reviewer for comments on a previous version of this manuscript.

References

Adams, W. P., Areal differentiation of snow cover in east central Ontario, *Water Resour. Res.*, *12*, 1226–1234, 1976.

Ahrens, C. D., *Meteorology Today*, 591 pp., West Publ., Eagan, Minn., 1994.

Akima, H., A new method of interpolation and smooth curve fitting based on local procedures, *J. Assoc. Comput. Mach.*, *17*, 589–602, 1970.

Carroll, T., *Airborne Gamma Radiation Snow Survey Program: A User's Guide, Version 5.0*, Natl. Oper. Hydrol. Remote Sens. Cent., Chanhassen, Minn., 2001.

Chang, A. T. C., J. L. Foster, and D. K. Hall, Satellite sensor estimates of Northern Hemisphere snow volume, *Int. J. Remote Sens.*, *11*, 167–171, 1990.

Chang, A. T. C., J. L. Foster, and A. Rango, Utilization of surface cover composition to improve the microwave determination of snow water equivalent in a mountain basin, *Int. J. Remote Sens.*, *12*, 2311–2319, 1991.

Chang, A. T. C., J. L. Foster, and D. K. Hall, Effects of forest on the snow parameters derived from microwave measurements during the BOREAS Winter Field Campaign, *Hydrol. Processes*, *10*, 1565–1574, 1996.

Cline, D. W., Snow surface energy exchanges and snowmelt at a continental, midlatitude alpine site, *Water Resour. Res.*, *33*, 689–701, 1997.

Cline, D., and T. Carroll, SNOW-INFO development and implementation plan, 22 pp., Natl. Oper. Remote Sens. Cent., Off. of Hydrol., Natl. Weather Serv., Silver Spring, Md., 1999.

Davis, R. E., A. W. Nolin, R. Jordan, and J. Dozier, Towards predicting temporal changes of the spectral signatures of snow in visible and near-infrared wavelengths, *Ann. Glaciol.*, *17*, 142–148, 1993.

Derksen, C., E. LeDrew, A. Walker, and B. Goodison, Winter season variability in North American prairie SWE distribution and atmospheric circulation, *Hydrol. Processes*, *14*, 3273–3290, 2000a.

Derksen, C., E. LeDrew, and B. Goodison, Temporal and spatial variability of North American prairie snow cover (1988–1995) inferred from passive-microwave derived snow water equivalent imagery, *Water Resour. Res.*, *36*, 255–266, 2000b.

Derksen, C., E. LeDrew, A. Walker, and B. Goodison, Influence of sensor overpass time on passive microwave-derived snow cover parameters, *Remote Sens. Environ.*, *71*, 297–308, 2000c.

Ellis, A. W., and D. J. Leathers, Analysis of cold air mass temperature modification across the U.S. Great Plains as a consequence of snow depth and albedo, *J. Appl. Meteorol.*, *38*, 696–711, 1999.

Frei, A., D. A. Robinson, and M. G. Hughes, North American snow extent: 1900–1994, *Int. J. Clim.*, *19*, 1517–1534, 1999.

Goodison, B. E., Accuracy of snow samplers for measuring shallow snowpacks, an update, in *Proceedings of the 35th Annual Eastern Snow Conference*, pp. 36–49, 1978a.

Goodison, B. E., Snowfall and snow cover in southern Ontario: Principles and techniques of assessment, Ph.D. thesis, Univ. of Toronto, Toronto, Ont., Canada, 1978b.

Goodison, B. E., Determination of areal snow water equivalent on the Canadian prairies using passive microwave satellite data, in *Proceedings of the International Geoscience and Remote Sensing Symposium*, vol. 3, pp. 1243–1246, IEEE Press, Piscataway, N. J., 1989.

Goodison, B. E., and A. E. Walker, Canadian development and use of snow cover information from passive microwave satellite data, in *Passive Microwave Remote Sensing of Land-Atmosphere Interactions*, edited by B. J. Choudhury et al., pp. 245–262, VSP BV, Utrecht, Netherlands, 1995.

Goodison, B., I. Rubinstein, F. Thirkettle, and E. Langham, Determination of snow water equivalent on the Canadian prairies using microwave radiometry, in *Modelling Snowmelt Induced Processes: Proceedings of the Budapest Symposium*, pp. 163–173, Int. Assoc. of Hydrol. Sci., Wallingford, England, 1986.

Grody, N., and A. Basist, Global identification of snow cover using SSM/I measurements, *IEEE Trans. Geosci. Remote Sens.*, *34*, 237–249, 1996.

Grundstein, A. J., and D. J. Leathers, A case study of the synoptic patterns influencing midwinter snowmelt across the northern Great Plains, *Hydrol. Processes*, *12*, 2293–2305, 1998.

Hall, D. K., J. L. Foster, and A. T. C. Chang, Measurement and modeling of microwave emission from forested snowfields in Michigan, *Nordic Hydrol.*, *13*, 129–138, 1982.

Idso, S. B., A set of equations for full spectrum and 8- to 14-um and 10.5- to 12.5-um thermal radiation from cloudless skies, *Water Resour. Res.*, *17*(2), 295–304, 1981.

Jordan, R., A one-dimensional temperature model for a snow cover: Technical documentation for SNTHERM.89, *Spec. Rep. 91-16*, U.S. Army Cold Reg. Res. and Eng. Lab., Hanover, N. H., 1991.

Kukla, G., and D. A. Robinson, Accuracy of operational snow and ice charts, *IEEE Int. Geosci. Remote Sens. Symp.*, 974–987, 1981.

Larson, L. W., Shielding precipitation gauges from adverse wind effects with snow fences, *Water Resour. Ser. 25*, Univ. of Wyo., Laramie, 1971.

Legates, D. R., and T. L. DeLiberty, Precipitation measurement biases in the United States, *Water Resour. Bull.*, *29*, 855–861, 1993.

Lynch-Stieglitz, M., The development and validation of a simple snow model for the GISS GCM, *J. Clim.*, *7*, 1842–1855, 1994.

Marshall, S. E., and S. G. Warren, Parameterizations of snow albedo for climate models, *Int. Assoc. Hydrol. Sci.*, *166*, 43–50, 1987.

Mote, T. L., and M. R. Anderson, Variations in melt on the Greenland Ice Sheet based on passive microwave measurements, *J. Glaciol.*, *41*, 51–60, 1995.

National Climatic Data Center, Summary of the day, first order, *TD-3210*, Asheville, N. C., 2000a.

National Climatic Data Center, Surface Land Daily Cooperative, Summary of the day, *TD-3200*, Asheville, N. C., 2000b.

National Snow and Ice Data Center, NOAA/NASA Pathfinder SSM/I level 3 EASE-grid brightness temperatures, Distrib. Active Arch. Cent., Univ. of Colo., Boulder, 1999.

National Weather Service, *National Weather Service Observing Handbook No. 7: Surface Weather Observations and Reports*, part IV, *Supplemental Observations*, 57 pp., Silver Spring, Md., 1996.

Rosenberg, N. J., B. L. Blad, and S. B. Verma, Microclimate: The Biological Environment, 495 pp., John Wiley, Hoboken, N. J., 1983.

Rowe, C. M., K. C. Kuivinen, and R. Jordan, Simulation of summer snowmelt on the Greenland ice sheet using a one-dimensional model, *J. Geophys. Res.*, *100*, 16,265–16,273, 1995.

Schmidlin, T. W., Assessment of NWS surface-measured snow water equivalent data based on remotely-sensed data in the northern Plains, in *Proceedings of the 46th Eastern Snow Conference*, pp. 208–212, 1989.

Schmidlin, T. W., A critique of the climatic record of "water equivalent of snow on the ground" in the United States, *J. Appl. Meteorol.*, *29*, 1136–1141, 1990.

Schmidlin, T. W., D. S. Wilks, M. McKay, and R. P. Cember, Automated quality control procedure for the "water equivalent of snow on the ground" measurement, *J. Appl. Meteorol.*, *34*, 143–151, 1995.

Shapiro, R., A simple model for the calculation of the flux of direct and diffuse solar radiation through the atmosphere, *Rep. AFGL-TR-0200*, Air Force Geophys. Lab., Bedford, Mass., 1987.

Tait, A. B., Estimation of snow water equivalent using passive microwave radiation data, *Remote Sens. Environ.*, *64*, 286–291, 1998.

Walker, A. E., and B. E. Goodison, Discrimination of a wet snow cover using passive microwave satellite data, *Ann. Glaciol.*, *17*, 307–311, 1993.

Wilson, L. L., L. Tsang, J. N. Hwang, and C. T. Chen, Mapping snow water equivalent by combining a spatially distributed snow hydrology model with passive microwave remote-sensing data, *IEEE Trans. Geosci. Remote Sens.*, *37*(2), 690–704, 1999.

Yang, D., B. E. Goodison, S. Ishida, and C. S. Benson, Adjustment of daily precipitation data at 10 stations in Alaska: Application of World Meteorological Organization intercomparison results, *Water Resour. Res.*, *34*, 241–256, 1998.

Yang, D., et al., Quantification of precipitation measurement discontinuity induced by wind speeds on national gauges, *Water Resour. Res.*, *35*(2), 491–508, 1999.

Yang, Z.-L., R. E. Dickinson, A. Robock, and K. Vinnikov, Validation of the snow submodel of the Biosphere-Atmosphere Transfer Scheme with Russian snow cover and meteorological observational data, *J. Clim.*, *10*, 353–373, 1997.

A. J. Grundstein and T. L. Mote, Climatology Research Laboratory, Department of Geography, University of Georgia, Athens, GA 30602, USA. (tmote@uga.edu)

D. J. Leathers, Center for Climatic Research, Department of Geography, University of Delaware, Newark, DE 19716, USA.

D. A. Robinson, Department of Geography, Rutgers University, Piscataway, NJ 08854, USA.